BioscienceHorizons Volume 3 • Number 1 • March 2010
10.1093/biohorizons/hzq008
Advance Access publication 27 February 2010

Research article

A study of the dynamics behind methane emissions from northern wetlands

Stuart Nattrass*

University of York, York, UK.

* **Corresponding author:** 207 Wolfson House, Stephenson Way, Euston, London, NW1 2HE, UK. Tel: +44 20 7679 5033. Email: stunattrass@googlemail.com

Supervisor: Dr Jon Pitchford, University of York, York, UK.

Methane is an important greenhouse gas, contributing 22% to the increased radiative forcing over 150 years, and emissions from wetlands are key to its global dynamics. A general model of methane dynamics is presented that emphasizes the impact of external climate factors on methane production and oxidation. The model consists of two uncoupled bacterial populations, each following a logistic growth pattern, and a third differential equation, dependent on these two populations, that represents the concentration of stored methane in wetland soils. This is related to methane emissions into the atmosphere. Several simplified models are also presented to demonstrate the development of the model from the basic processes occurring in the soil. Analysis of the model shows a stable equilibrium point for the methane concentration. This equilibrium is subject to short-term forcing by climate, specifically changes in temperature and water table depth. Parameters for this model are then fitted to real data taken from a wetland site in Teesdale, and this forcing is shown to account for much of the observed variation in methane emissions. An attempt to extend this model to longer time scales is made, by considering the average climate. This extension is shown to be unsuccessful through considering Taylor's theorem and its implications for the model. Finally, a simplistic approximation to climate change is made, and the consequences of these changes on methane emissions predicted by the model are presented. These consequences are found to include negative feedback, where the change in climate eventually results in lower emissions of methane.

Key words: methane, emissions, model, wetlands, climate, change.

Submitted on 19 September 2009; accepted on 6 January 2010

Introduction

Methane (CH_4) is a very potent greenhouse gas, roughly 25 times as strong as carbon dioxide.[1] This means it is an important factor when considering climate change, contributing ~22% of the global greenhouse effect.[2] Wetlands are the source of over 40% of annual global methane emissions,[3] so an understanding of the emissions from these areas is crucial to furthering our understanding of climate change. In order to predict the probable effects of climate change, a model that accurately predicts methane emissions is required. This would allow accurate simulations of methane flux into the future, in turn presenting opportunities to affect policy and the management of greenhouse gas emissions.

This article aims to construct a simple mathematical model based primarily on the effects of external factors such as climate, but also considering the implications of laboratory work on the biochemical factors involved. The model dynamics are considered, and the response to increased temperature and precipitation, according to projected trends, is simulated. The objective was to accurately represent the emissions of methane from the wetland environment and study the consequences of realistic assumptions on emissions over a period of ~300 years. This 300-year time period is arbitrary, but it illustrates an important change in the system's dynamics; a transition from positive to negative feedback.

Model development

A simple model

Any model of methane emissions from wetlands must take into account the three main processes within the soil.

These are methane production in anaerobic conditions, methane oxidation in aerobic conditions and the flux of methane from the soil into the atmosphere.[4] Clearly, production increases soil methane concentrations, whereas the other processes reduce methane concentration in the soil.

The production of methane is highly dependent on soil temperature,[4] as increased temperature results in an increase in soil temperature. This dependence takes a well-documented exponential form, so that production P satisfies

$$P(T) = pQ_{10}^{(T-T_m)/10}, \tag{1}$$

for constant p, temperature T and the average temperature T_m, at which the rate of production is known or can be calculated. The constant Q_{10} determines how rapidly production increases with temperature. However, by also considering the underlying biochemistry, we can make our model more realistic. Production occurs when methanogenic bacteria facilitate the following two chemical reactions:

$$CH_3COOH \rightarrow CH_4 + CO_2, \tag{2}$$

$$CO_2 + 4H_2 \rightarrow CH_4 + 2H_2O. \tag{3}$$

We assume that the archaea facilitate these reactions in accordance with the law of mass action, so that a reaction $A + B \rightarrow C$ occurs at a rate proportional to $[A][B]$, where $[X]$ denotes the concentration of substance X. Because the reactions are dependent on the presence of methanogens, we assume the rate to be proportional to the methanogen biomass. This results in the production term of our model becoming

$$P = pQ_{10}^{(T-T_m)/10}B_{mg}([CH_3COOH] + [CO_2][H_2]^4). \tag{4}$$

Here, B_{mg} is the methanogenic biomass and p a constant representing the effectiveness of the bacteria facilitating the reaction.

Similarly, bacteria, this time methanotrophic, facilitate the oxidation of methane in aerobic soils, via the following reaction:

$$CH_4 + 2O_2 \rightarrow CO_2 + 2H_2O. \tag{5}$$

Again, we assume the reaction to adhere to the law of mass action, and also for the rate to be proportional to the methanotrophic bacterial biomass, which is denoted by B_{mt}. It has also been shown[5] that decomposition has a similar temperature dependence to production. However, temperature has much less effect on oxidation,[5] and so we denote the temperature dependence constant by q_{10}. Combining this with the law of mass action acting on the oxidation equation, we get a decomposition term of

$$R = kq_{10}^{(T-T_m)/10}B_{mt}[CH_4][O_2]^2. \tag{6}$$

This leaves transfer of methane from the soil to the atmosphere. There are three main forms for this to occur: diffusion across the soil–air boundary; ebullition—where methane bubbles up through the soil; and plant-mediated transport. Diffusion occurs across concentration gradients, and because the concentration of methane in the atmosphere is so low, we assume diffusion to be proportional to the soil methane concentration. Both ebullition and plant-mediated transport are also dependent on the amount of methane in the soil, so both these are set proportional to the soil methane concentration. As such the flux from soil to atmosphere is given simply by a constant U multiplied by the soil methane concentration. Combining this with the production and oxidation terms, we get

$$\frac{d[CH_4]}{dt} = pQ_{10}^{(T-T_m)/10}B_{mg}([CH_3COOH] + [CO_2][H_2]^4) - kq_{10}^{(T-T_m)/10}B_{mt}[CH_4][O_2]^2 - U[CH_4], \tag{7}$$

where the values of all substance concentrations except methane are kept constant to preserve simplicity.

We also introduce variable bacterial dynamics for each of the populations. Taking the biomass to follow the logistic model, we get

$$\frac{dB_{mg}}{dt} = r_{mg}B_{mg}\left(1 - \frac{B_{mg}}{\alpha}\right), \tag{8}$$

$$\frac{dB_{mt}}{dt} = r_{mt}B_{mt}\left(1 - \frac{B_{mt}}{\beta}\right), \tag{9}$$

where r_{mg} and r_{mt} are the respective growth rates of B_{mg} and B_{mt}, when there is no competition and resources (in this case, substrate) are plentiful, and α and β are the maximum biomasses that can be sustained by the environment. These are considered constant in the current model to preserve simplicity.

Phase portrait analysis

We now have a three-dimensional model given by Equations (7–9). However, the equation for B_{mt} is uncoupled, with an unstable fixed point at $B_{mt} = 0$ and a stable fixed point at $B_{mt} = \beta$. We can now simplify our model by noting that methanotrophic bacteria reproduce much faster than methanogens, with a typical growth rate between 14% and 34% per hour,[6] as opposed to 40% per day for methanogens.[7] We can therefore assume that the methanotrophs reach their equilibrium point much faster, and so we can consider them as a constant β. This reduces our model to a two-

dimensional problem. We then further simplify it by transforming the equations into a dimensionless form. Setting

$$[CH_4] = \sqrt{\frac{\alpha}{r_{mg}}}\frac{pQ_{10}^{(T-T_m)/10}\left([CH_3COOH] + [CO_2][H_2]^4\right)}{kq_{10}^{(T-T_m)/10}\beta[O_2]^2 + U}x, \quad (10)$$

$$B_{mg} = \sqrt{\frac{\alpha}{r_{mg}}}y, \quad (11)$$

$$t = \frac{1}{kq_{10}^{(T-T_m)/10}\beta[O_2]^2 + U}\tau, \quad (12)$$

and labelling $kq_{10}^{(T-T_m)/10}\beta[O_2]^2 + U = b$, and differentiating with respect to τ, we get the simplified dynamical system

$$\frac{dx}{d\tau} = y - x, \quad (13)$$

$$\frac{dy}{d\tau} = \frac{r_{mg}}{b}y - y^2. \quad (14)$$

The fixed points for this system are at $(x, y) = (0, 0)$ and $(x, y) = (r_{mg}/b, r_{mg}/b)$. Using linear stability analysis, we see that the origin is a saddle point, with stable manifold along the x-axis, and unstable manifold with positive slope along the eigenvector $(1, (r_{mg} + b)/b)$. The second fixed point, $(r_{mg}/b, r_{mg}/b)$, is a stable node for $r_{mg} \neq b$. There is a heteroclinic trajectory leaving the saddle point along the unstable manifold, tending to the stable node. The phase portrait for this system is shown in Fig. 1.

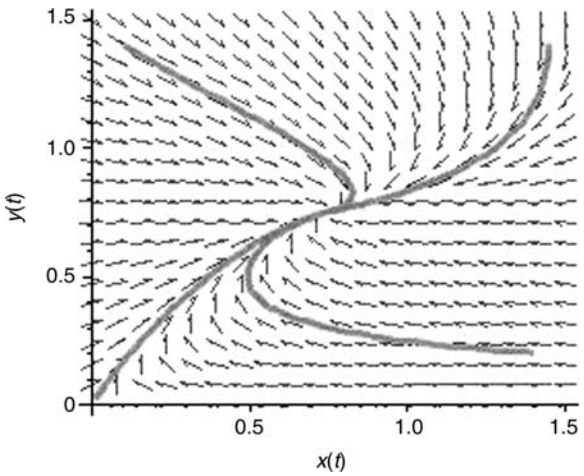

Figure 1. Phase portrait of the system given by Equations (7) and (8). Included are the heteroclinic orbit from the saddle at the origin to the stable node at $(r_{mg}/b, r_{mg}/b)$, and three other trajectories exemplifying the global stability of the node. Parameter values are $r_{mg} = 3$ and $b = 4$, which are not based on data but demonstrate the general behaviour sufficiently.

Once the system reaches the equilibrium point with concentration $[CH_4]^*$, the flux is given by

$$\text{Flux} = U[CH_4]^* = U\frac{pQ_{10}^{(T-T_m)/10}\alpha\left([CH_3COOH] + [CO_2][H_2]^4\right)}{kq_{10}^{(T-T_m)/10}\beta[O_2]^2 + U}, \quad (15)$$

where $[CH_4]^*$ is found by setting Equation (7) equal to zero.

Climate forcing

Until now, we have operated with the assumption of a constant climate. This is clearly a gross simplification, and so now we look to introduce climate forcing. Figure 2 shows temperatures for each day throughout 1995 at the Moorhouse site in Teesdale. The figures are reached by recording the temperatures daily at the surface, and at depths of 10, 30 and 100 cm, and taking the average of the four. We use the average as we are not considering the spatial distribution of resources within the soil. We now make the simplifying assumption that the soil processes on day i are only affected by the climate on day i, so that the temperature and water table from the previous days have no effect on the flux. A further initial assumption, taking our lead from other wetland studies,[8] is that all dynamics are fast, so both bacterial biomasses and methane concentration track at their respective equilibrium values.

However, temperature is not the only important climate factor to consider. We have assumed thus far that water table depth has no effect. However, this approximately marks the boundary between the anaerobic soil, where production primarily occurs, and the aerobic area of the soil, where oxidation occurs.[9] Figure 3 shows the depth of the water table throughout 1995. As such, we now assume that production occurs exclusively below the water table,

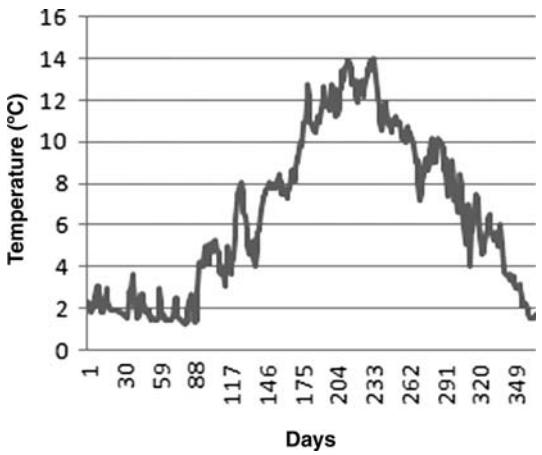

Figure 2. Soil temperature at the Moorhouse site throughout 1995. The value displayed is an average of the recorded temperature at four different depths.

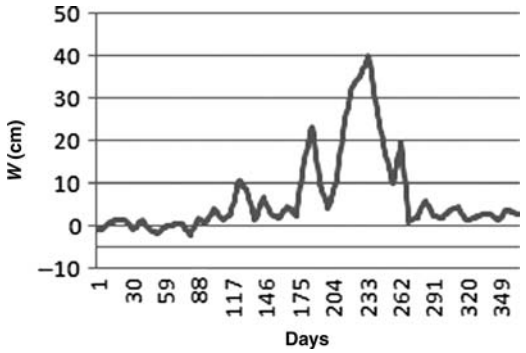

Figure 3. The depth below the surface of the water table at Moorhouse through 1995. Negative value indicates surface water.

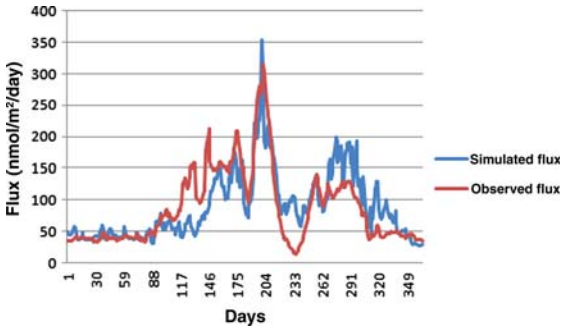

Figure 4. Simulation of the flux model (17), alongside observed flux at the Moorhouse site. Parameter values are $p = k = 2.5$, $\alpha = 900$, $[S] = 0.36$, $[O_2] = 0.3$, $U = 0.9$, $Q_{10} = 14.75$, $q_{10} = 1.4$, $T_m = 6.5$, $\gamma = 20$ and $c = 0.2$.

whereas oxidation is restricted to the aerobic area between the surface and the water table. Studies have shown that methane fluxes controlled by conditions close to the surface and are not affected by production at lower levels. As such, we assume that production occurs in an area of constant size below the water table, allowing us to retain a constant methanogen carrying capacity α. However, methanotrophs require oxic soil, so if the water table is at or above the surface, little or no oxidation can occur. When the water table is below the surface, these bacteria can facilitate the oxidation of methane. Also, there are small areas of aerobic soil around plant roots that supplied oxygen via the plant, even when surrounded by saturated soil. This results in a methanotrophic-carrying capacity that is dependent on water table depth. Assuming that the bacteria are spread evenly throughout the soil, we get a linear relationship, such that

$$\beta = \gamma(1 + cW), \tag{16}$$

where W is the maximum of 0 and w, the distance down from the surface to the water table, γ determines the amount of oxidation when the whole soil profile is saturated and c is a scaling constant reflecting the amount of bacteria the environment can sustain in an area of 1 cm depth.

Assuming that our model tracks the equilibrium (i.e. assuming that the ecological dynamics are sufficiently fast) gives us the new flux model

$$\text{Flux} = F = U\frac{pQ_{10}^{(T-T_m)/10}\alpha[S]}{kq_{10}^{(T-T_m)/10}\gamma(1 + cW)[O_2]^2 + U}, \tag{17}$$

where the notation is simplified by setting $([CH_3COOH] + [CO_2][H_2]^4) = [S]$.

Selecting the parameters from within the ranges in the literature, the value of Equation (17) was then calculated for the temperature and water table depth of each day during 1995. This simulation, along with the observed methane emissions from the site, is shown in Fig. 4. From the figure, we can see that our model does indeed qualitatively mirror the observed data, predicting high emissions, where high emissions were observed, and low emissions, where the recorded flux was lower. However, we must note that our model does not decrease as much as the observed flux between days 200 and 240. Figure 3 shows that this period, days 200–240, is when the water table is deepest below the surface, suggesting that our model overestimates the flux when the water table is deep. We also note that our model underestimates flux during much of spring, suggesting that there are more factors and processes to be considered.

Root-facilitated methane production

The model outlined above limits methane production to a zone just below the water table, where conditions are anaerobic. However, methane is also produced above the water table around plant roots, where soil oxidation is incomplete,[4] all be it to a lesser extent than in fully anaerobic conditions. We assume that this root-facilitated production involves the same archaea that operate below the water table, and that the amount of roots in aerobic conditions increases linearly as the water table falls below the surface. However, as this process occurs in partially oxidized soil, we assume that the presence of oxygen is a greater factor in limiting production than in fully anaerobic condition, where temperature seems to be the key limitation on production. This is characterized by a different temperature dependence for production around roots, denoted by $\hat{Q}_{10}$.

This results in a second production term in our dynamical system, representing the root-facilitated production. Production P is now given by

$$P = \left(pQ_{10}^{(T-T_m)/10} + w\hat{p}\hat{Q}_{10}^{(T-T_m)/10}\right)B_{mg}[S], \tag{18}$$

where $\hat{p}$ is defined similarly to p as the production rate around roots at temperature T_m. Substituting this into

Equation (7) gives

$$\frac{\mathrm{d}[\mathrm{CH_4}]}{\mathrm{d}t} = \left(pQ_{10}^{(T-T_\mathrm{m})/10} + w\hat{p}\hat{Q}_{10}^{(T-T_\mathrm{m})/10}\right)B_\mathrm{mg}[\mathrm{S}] - kq_{10}^{(T-T_\mathrm{m})/10}B_\mathrm{mt}[\mathrm{CH_4}][\mathrm{O_2}]^2 - U[\mathrm{CH_4}], \quad (19)$$

which when taken to equilibrium gives a flux model

$$F = U\frac{\left(pQ_{10}^{(T-T_\mathrm{m})/10} + w\hat{p}\hat{Q}_{10}^{(T-T_\mathrm{m})/10}\right)\alpha[\mathrm{S}]}{kq_{10}^{(T-T_\mathrm{m})/10}\gamma(1+cW)[\mathrm{O_2}]^2 + U}. \quad (20)$$

Flux with extreme water table

We now return to the earlier observation that the response of our model to a deep water table appears weaker than required. Previously, we represented flux by Equation (17), where the relationship between flux and water table depth was qualitatively equivalent to $F = (1 + W)^{-1}$, where $W = \max(0, w)$ as previously, which for large w behaves like $1/w$. By introducing root-facilitated methanogenesis in Equation (20), our model now acts like $F = (a + w)/(1 + W)$, which for large w approximates the constant 1. This does not, however, match the dip in observed flux when w is large.

Indeed, plotting the observed flux against water table depth w, as shown in Fig. 5, suggests that the functional response of flux to varying water table depth is similar to $F = (a + w)/(1 + bW^s)$, for constants b and $s > 1$. When $s = 2$, this looks like $1/w$ for large w, which earlier seemed to underestimate the effect of a deep water table. Setting $s = 3$, and approximating the functional response such that the y-intersect is at 40 nmol, and the function peaks around $w = 6.5$, with maximal flux 270 nmol of methane, we find that flux decreases more rapidly than the observed data for large w. Thus, we select s in the open interval (2,3), choosing $s = 5/2$.

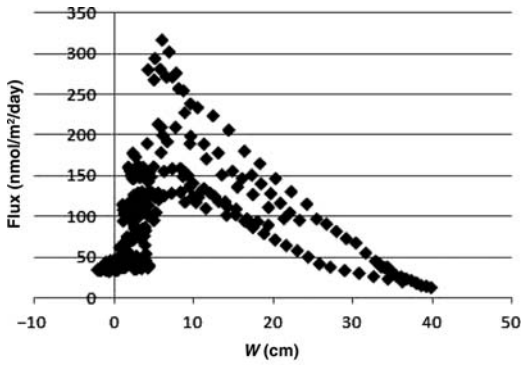

Figure 5. Observed methane flux from the Moorhouse site plotted against water table depth.

Transferring this back to our model, we can explain this by noting that bacteria are not evenly spread throughout the soil profile and are less prevalent near the surface than in deeper layers.[10] Thus, we assume that methanotrophic biomass increases as we go down the soil profile, so aerobic oxidation occurs at a rate proportional to $W^{5/2}$, replacing Equation (9) with

$$\frac{\mathrm{d}B_\mathrm{mt}}{\mathrm{d}t} = r_\mathrm{mt}B_\mathrm{mt}\left(1 - \frac{B_\mathrm{mt}}{\gamma(1+cW^{5/2})}\right), \quad (21)$$

giving a stable attractor at $B_\mathrm{mt} = \gamma(1 + cW^{5/2})$.

Here, we also note that while there is no change in the amount of oxidation when there is surface water, the flux is affected. This is because surface water can retain methane without releasing it into the atmosphere. We assume that this occurs linearly, and incorporate it into our model by allowing 'negative production' around plant roots. Clearly, this is not what actually happens, but allows us to include this factor while keeping the model as simple as possible. Therefore, our flux model now looks like

$$F = U\frac{\left(pQ_{10}^{(T-T_\mathrm{m})/10} + w\hat{p}\hat{Q}_{10}^{(T-T_\mathrm{m})/10}\right)\alpha[\mathrm{S}]}{kq_{10}^{(T-T_\mathrm{m})/10}\gamma(1+cW^{5/2})[\mathrm{O_2}]^2 + U}. \quad (22)$$

Parameter estimation

The next problem we face is finding parameters that are both biologically realistic and ensure that our model fits the observed data well. To achieve this, we use the techniques of non-linear regression, and in particular least squares analysis.[11] The aim of least-squares analysis is to reduce the χ^2 value, measuring the distance between observed data $f(i)$ and the prediction of a model $F(i)$.

In order to simplify the least squares analysis, we first reduce our flux model to a form containing the smallest number of parameters that can capture all the information in the model. Grouping constants together and labelling the new parameters a_i, we can reduce our model by defining new parameters as follows:

$$a_1 = pa[\mathrm{S}]Q_{10}^{-T_\mathrm{m}/10}, \quad (23)$$

$$a_2 = \ln Q_{10}, \quad (24)$$

$$a_3 = \hat{p}\alpha[\mathrm{S}]\hat{Q}_{10}^{-T_\mathrm{m}/10}, \quad (25)$$

$$a_4 = \ln \hat{Q}_{10}, \quad (26)$$

$$a_5 = \frac{k[\mathrm{O_2}]^2\gamma c}{U}q_{10}^{-T_\mathrm{m}/10}, \quad (27)$$

$$a_6 = \ln q_{10}, \quad (28)$$

$$a_7 = \frac{1}{c}, \quad (29)$$

which we can then arrange into a seven-dimensional vector $\boldsymbol{a}$, with ith parameter a_i.

Unfortunately, due to singularities that occur in $\partial F/\partial s$ whenever the water table is at or above the surface, we cannot use the method outlined below to estimate the parameter s. As such, we continue to use a default value of $s = 5/2$. Taking our seven parameters and rearranging, the daily flux model reduces to something a little simpler,

$$F(i|\boldsymbol{a}) = \frac{a_1 \exp(a_2 T(i)/10) + w(i) a_3 \exp(a_4 T(i)/10)}{1 + a_5 \exp(a_6 T(i)/10)(a_7 + W(i)^{5/2})}, \quad (30)$$

which still contains all the data of our model, and $F(i|a)$ is the flux on day i given a set of parameters a.

Once this simplification is made, we need a method of improving the fit of the model by adjusting the parameters. The method we choose to use is the Levenberg–Marquardt method of least squares analysis,[11] to minimize the χ^2 value. Define

$$B_i = \sum_{t=1}^{365} (f(t) - F(t|\boldsymbol{a})) \frac{\partial F(t|\boldsymbol{a})}{\partial a_i}, \quad (31)$$

giving a seven-dimensional vector **B**, and

$$A_{ij} = \begin{cases} \sum_{t=1}^{365} \frac{\partial F(t|\boldsymbol{a})}{\partial a_i} \frac{\partial F(t|\boldsymbol{a})}{\partial a_j}, & i \neq j \\ (1+\lambda) \sum_{t=1}^{365} \left(\frac{\partial F(t|\boldsymbol{a})}{\partial a_i} \right)^2, & i = j \end{cases}, \quad (32)$$

where all derivatives are evaluated at the point $\boldsymbol{a}$, and λ is chosen to be small, in our case 0.01. The A_{ij}'s are placed in a matrix A. The key stage in the algorithm is solving the equation

$$A\boldsymbol{d} = \boldsymbol{B}, \quad (33)$$

for the unknown vector $\boldsymbol{d}$. We then define $\bar{\boldsymbol{a}} = \boldsymbol{a} + \boldsymbol{d}$. If the χ^2 value for the model is lower with the new set of parameters $\bar{\boldsymbol{a}}$, then λ is reduced by a factor of 2, and we redefine $\boldsymbol{a}$ by $\boldsymbol{a} = \bar{\boldsymbol{a}}$ and repeat the process with the new parameters. If the χ^2 value increases with our change of parameters, then we double λ and repeat. We do this until χ^2 remains approximately constant, halting the process when it remains constant to a precision on four decimal places.

For an initial estimation of parameters, we choose $\boldsymbol{a}^{\mathrm{T}} = (35, 1.4, 10, 0.3, 0.0015, 0.1, 5)$. Running the algorithm once from this starting point returns $\boldsymbol{a}^{\mathrm{T}} \approx (23.1, 1.93, 1.3, 2.65, 0.0005, 1.71, 68.3)$. However, because λ is reduced by a factor of 2 every time we reduce the χ^2 value, the algorithm does not necessarily run to convergence. If the initial estimate is too far from the minimum we are seeking, the algorithm can stop while still a long way from the minimum. Note that in running the algorithm, a_6 has increased to more than 17 times its initial value, and a_7 has increased to almost 14 times the initial value. Because of this, we could still be a considerable distance from the χ^2 minimum. As such, we run the algorithm a second time, starting from the approximate endpoint of the first run given above. This second iteration gives

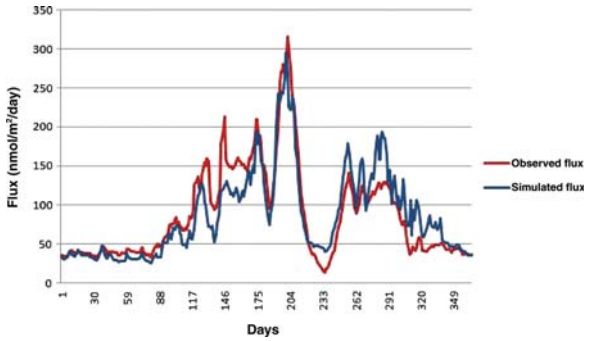

Figure 6. The simulated flux using Equation (30), with parameters given by Equation (34), plotted against observed values.

$$\boldsymbol{a}^{\mathrm{T}} \approx (23.8, 1.85, 1.31, 2.58, 0.000428, 1.78, 52.5). \quad (34)$$

which gives $\chi^2 \approx 250\,000$, rounded to three significant figures. None of the parameters have changed dramatically in the second iteration, so we take $\boldsymbol{a}$ to be our set of parameters.

Figure 6 shows that we do indeed have a better approximation of the real world data than in our previous model, which had $\chi^2 \approx 532\,000$, again rounded to three significant figures. Our new model captures all the general behaviour of the real data, if not the fine detail. We also note that while it is a much better fit for large w, it does still overestimate flux in this scenario.

We must, however, check that the parameters given in Equation (34) are biologically realistic. The parameters a_2, a_4, a_6 and a_7 immediately give $Q_{10} \approx 6.36$, $\hat{Q}_{10} \approx 13.2$, $q_{10} \approx 5.91$ and $c \approx 0.0191$, all rounded to three significant figures. This value of q_{10} is slightly higher than those found in the literature, although this could be because we were unable to optimize our parameter s, so we accept and continue to use this value. As before, we assume that 90% of produced methane is emitted, i.e. $U = 0.9$, and we now assume that 2 mg is the average amount of bacteria contained in a patch of soil 1 cm deep, i.e. $\gamma = 2$. We also assume that methane is produced up to a metre below the water table, returning $\alpha = 200$. Taking $[S] = 0.36$ and $[O_2] = 0.3$ from the literature,[10] some simple algebra returns production and oxidation rates $p \approx 10$, $\hat{p} \approx 0.0974$ and $k \approx 0.0612$, where these rates are given in units of nmol/day. The production is much lower around plant roots than in fully anaerobic conditions, as expected given the presence of oxygen as an inhibitor near roots. These parameters all seem biologically reasonable, except q_{10}, as already discussed, so we can confidently use the flux model given by Equations (30) and (34).

Discussion and analysis

Equilibrium assumptions

In developing our model, we have assumed that all dynamics are fast and that the model tracks at equilibrium for both bacterial biomasses and soil methane concentration. Indeed, B_{mg} has a constant stable attractor at $B_{mg}(t) = \alpha$. Since we are studying the wetland area long after it forms, we can safely continue to assume that the methanogenic biomass is at this fixed point by the time we come to model it. Then, by the definition of a fixed point, it remains there for all time.

The methanotrophic biomass, however, is pulled by the model towards a stable fixed point that moves with the water table depth. We suppose that the time during day i that measurements are taken represents time zero for a new logistic model, with carrying capacity $\beta = \gamma\left(1 + cW^{5/2}(i+1)\right)$.

We now note that the logistic equation can be solved analytically. Rearranging Equation (9) and integrating, we get

$$\int\left(\frac{1}{B_{mt}} + \frac{1}{\beta - B_{mt}}\right)dB_{mt} = \int r_{mt}dt, \tag{35}$$

which upon exponentiation gives the solution

$$B_{mt}(t) = \frac{\beta C\exp(r_{mt}t)}{1 + C\exp(r_{mt}t)}, \tag{36}$$

where c is a constant dependent on the initial condition, taken to be the methanotrophic biomass on day i. Setting $t = 0$ gives

$$C = \frac{B_{mt}(0)}{\beta + B_{mt}(0)}. \tag{37}$$

We now consider the implications of this for our methanotrophic biomass. We need to consider how quickly this model closes in on the stable equilibrium, as this will indicate whether we can continue to use equilibrium values when considering the flux model, or whether we need to consider the bacterial dynamics explicitly.

If we are to continue assuming fast dynamics, taking the equilibrium point on day i as the initial condition, and the next days equilibrium point as the carrying capacity, β should return $B_{mt}(1) \approx \beta$ for all i. It is easy to calculate

$$B_{mt}(1) = \frac{\beta C\exp(r_{mt})}{1 + C\exp(r_{mt})}, \tag{38}$$

so $B_{mt}(1) \approx \beta$ is equivalent to

$$1 \approx \frac{C\exp(r_{mt})}{1 + C\exp(r_{mt})}. \tag{39}$$

To calculate r_{mt}, we use the lowest growth rate reported, 14% per hour.[6] Thus, after 1 h, a biomass of 1 has become 1.14. Extending over 24 h, this original biomass of 1 becomes 1.14^{24}, giving $r_{mt} = 1.14^{24} - 1 \approx 22.2$. We then need to consider when C is minimal, as this is when the right-hand side of Equation (39) is furthest from 1. This occurs when the initial condition is smallest and β is largest. The maximum value of β is with the deepest water table, $w = 39.92$ cm, giving $\beta \approx 386$, and the smallest initial condition is $\gamma = 2$. This gives $C \approx 0.00516$, which when entered into the right-hand side of Equation (39) returns 1, even when rounded to seven significant figures. Therefore, the worst-case scenario is

$$|B_{mt}(1) - \beta| < 10^{-7}, \tag{40}$$

so $B_{mt}(1)$ is clearly close to β, and we shall continue to assume that the methanotroph biomass tracks at equilibrium.

This leaves the equilibrium assumption on the soil methane concentration itself. We are not so fortunate here, in that any analytical solution is much more complicated. As such, we do not attempt this here. Instead, we numerically solve the differential equation (19) using a backwards Euler method,[11] choosing this as it is an implicit method, usually stable with much larger step size than the simpler explicit methods. In fact, since Equation (19) is linear in $[CH_4]$, we can simplify the implicit method. Taking the backwards Euler method, given by $y(t + h) = y(t) + hy'(t + h)$, and replacing the arbitrary function $y(t)$ with our function $[CH_4](t)$, we can rearrange to get

$$[CH_4](t+h) = \frac{[CH_4](t) + h\left(p\mathcal{Q}_{10}^{(T-T_m)/10} + w\hat{p}\hat{\mathcal{Q}}_{10}^{(T-T_m)/10}\right)\alpha[S]}{1 + h\left(kq_{10}^{(T-T_m)/10}B_{mt}[O_2]^2 + U\right)}. \tag{41}$$

For an initial condition for our simulation, we assume that at day 0, the temperature and water table depth are both at zero, and take the methane concentration to be the equilibrium value for this climate. We also assume that between measurements, the temperature and water table move linearly to the next observed level, so, for example, if $T(t) = a$ and $T(t + 1) = b$, then $T(t + 1/2) = (a + b)/2$. We then run a simulation of the soil methane concentrations throughout 1995 using this backwards Euler method, with step size $h = 1/2$. The daily flux is then calculated by multiplying the soil methane concentration by U. This is then plotted against the equilibrium flux on each day, as shown in Fig. 7. The figure shows that the results are very similar, with $r^2 = 0.9894$. We can also easily calculate the average discrepancy between the two models as 3.75 nmol/day, compared with average flux of 865 nmol/day. Because the equilibrium flux assumption affects the model's output so little and is simpler to work with, we continue assuming that all dynamics are fast.

Temporal scaling, Jensen's inequality

We now move on to look at the methane flux over longer time periods, in order to study the potential effects of

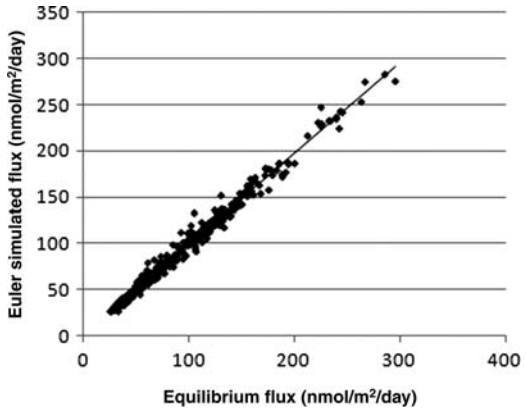

Figure 7. Plot of the backwards Euler simulation values plotted against the equilibrium flux values, with $r^2 = 0.9894$.

climate change on methane emissions. This would be much simpler if we just consider the average daily flux over a year and ignore the day-to-day variation. The average flux of our model is

$$\frac{1}{365}\sum_{t=1}^{365} F = U\frac{\left(pQ_{10}^{(T(t)-T_m)/10} + w(t)\hat{p}\hat{Q}_{10}^{(T(t)-T_m)/10}\right)\alpha[S]}{kq_{10}^{(T(t)-T_m)/10}\gamma(1+cW(t)^{5/2})[O_2]^2 + U} \approx 86.5. \tag{42}$$

However, it would simplify things greatly if we could consider this average flux in terms of the average climate. The simplest way to do this is to calculate the flux on a fictional day which has exactly average water table depth and temperature. In our case, though, this gives an average flux of 104 nmol/day, an obvious overestimation. This is an example of Jensen's inequality, expanded into two dimensions. Jensen's inequality states that in general, for a random variable X, and a function f, $\mathbf{E}(f(X)) \neq f(\mathbf{E}(X))$. Extended into two dimensions, this becomes

$$\mathbf{E}(f(X,Y)) \neq f(\mathbf{E}(X),\mathbf{E}(Y)), \tag{43}$$

for a second random variable Y.[12] The conventional approach in this situation is to take a Taylor's series expansion around the point $\mu = (\bar{X},\bar{Y})$, where $\bar{\cdot}$ is shorthand for the expectation operator $\mathbf{E}(\cdot)$. Taking a second-order Taylor's expansion, dropping the remainder and working out, expected values return

$$\mathbf{E}(f(X,Y)) \approx f(\mu) + \frac{\mathrm{Var}(X)}{2}\frac{\partial^2 f}{\partial X^2}(\mu) + \frac{\mathrm{Var}(Y)}{2}\frac{\partial^2 f}{\partial Y^2}(\mu) + \frac{\mathrm{Cov}(X,Y)}{2}\frac{\partial^2 f}{\partial X\partial Y}(\mu). \tag{44}$$

How good an approximation this is is determined by how non-linear the function f is. In our case, setting $X = T$, $Y = w$ and $f = F$ gives an average daily flux of 61.6 nmol. Whereas the first-order approximation overestimates the flux, this second-order approximation underestimates the emissions.

The natural extension here is to take higher-order approximations by extending the Taylor series to include higher derivatives. However, Taylor's theorem states that if a function f is n-times continuously differentiable on the interval $(X,\bar{X})$, and $(n+1)$-times differentiable, then the Taylor series expansion can only be guaranteed to converge to the function up to the nth-order approximation. We note that while our flux model F is smooth with respect to temperature, it is only piecewise smooth with respect to water table depth, as the function is different for $w > 0$ than for $w \leq 0$. Differentiating with respect to w three times, we see that the third derivative has a discontinuity at zero, as $\lim_{w\to 0^-} F^{(3)}(w) = 0$, but $\lim_{w\to 0^+} F^{(3)}(w) = -\infty$. Therefore, we can only guarantee convergence of the Taylor series up to the second derivatives. Extending this to two dimensions again, we can indeed see that the series does diverge, as the next two approximations are 12.9 and 187 nmol/day, both of which are much further from the actual average flux than earlier attempts. Thus, we now rule out the possibility of approximating the average flux in this manner.

Effects of climate change

Having ruled out the use of average climate, we must consider how to implement climate change trends into the model. Average global temperature is predicted to rise 2°C before the year 2100,[1] a rate of 0.02°C/year. The simplest way to implement this is to artificially increase the recorded temperature each day by 0.02°C. Another likely effect of climate change in the UK is increased precipitation. We assume that average precipitation increases by 0.2 cm/year. However, it is likely that this will be partially offset by increased evapotranspiration and runoff, so we assume that $\bar{w}$ decreases by 0.04 cm/year. Again, the simplest way to implement this is to artificially decrease w by 0.04 cm each day. Therefore, the average flux in year N is calculated by replacing $T(t)$ and $w(t)$ in Equation (42) by $T(t) + 0.02N$ and $w(t) - 0.04N$, respectively.

Figure 8 shows the average daily emissions each year until 2300, assuming the trends above continue. This shows that initially, the increase in temperature will cause higher emissions, overriding the decrease in w, which should cause emissions to drop. However, in year 150 of the simulation (2145), when $\bar{T} = 9.55$°C and $\bar{w} = 0.81$ cm, we reach a maximum flux, ~108 nmol/day. After this, the heightened water table becomes a more important factor than the increased temperature, and the emissions begin to drop, falling to approximately half current levels by 2300, when flux is 45.1 nmol/day.

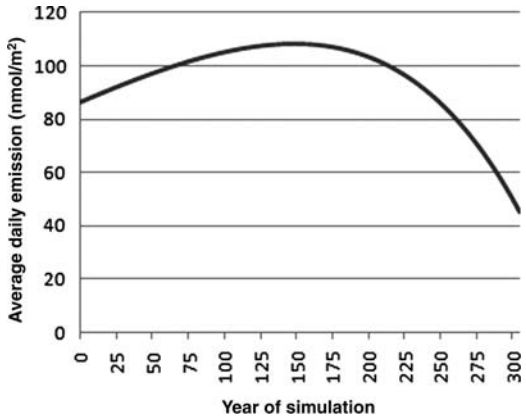

Figure 8. The average daily emissions for each year until 2300. The plot assumes that current climate change trends hold throughout the period.

Conclusion

The simple model above is based on a conceptual approach, built on the assumption that temperature and water table depth are important factors in determining methane emissions. This conceptual model is compared with observed data from the Moorhouse site in Teesdale and modified to better approximate the observed emissions. Although the model is much simplified, it captures the general patterns of methane flux, although does not capture fine details. This could possibly be improved by considering factors such as substrate concentration as dynamic, rather than the constants considered here. Further improvements could be including temperature dependence on plant-mediated transport,[13] or food dependence of bacterial carrying capacities, as growth rates are unlikely to be affected (K. Redeker, personal correspondence). Improved data fitting could be achieved by optimization of the parameter s, possibly using maximum-likelihood estimation. The model should also be checked against data from other wetland sites, possibly varying substrate concentration and bacterial biomass parameters.

Having approximated emissions, the implications of current climate change trends were considered. Initially, the emissions increased with temperature, due to methane potency as a greenhouse gas. However, 150 years into the simulation, flux begins to decrease. These predictions could be compared with observed flux in the future, although a more informative approach may be to consider the model outlined here integrated into a model describing peatland evolution.[8] This is an area that could lead to interesting work in the future.

Acknowledgements

Thanks must be given to Jon Pitchford (York Centre for Complex Systems Analysis (YCCSA), University of York) for his patience and guidance throughout the supervision of this project. I am also indebted to Kelly Redeker (Department of Biology, University of York) for providing biological insight, as well as Steve Palmer (School of Biological Sciences, University of Aberdeen) and Jamie Wood (YCCSA, University of York) for their enlightening discussions. Data were gratefully received from the Environmental Change Network.

Author biography

Stuart Nattrass has just finished an MMath Mathematics degree from the University of York, graduating with first class honours with distinction. During the course, he focussed on the areas of Number Theory and Dynamical Systems, discovering Mathematical Biology through the latter. His main interests are concerned with modelling evolution, biodiversity and climate change. His future plans include a PhD in Genetics and Evolution at University College London, and climbing Mount Kilimanjaro.

References

1. IPCC Fourth Assessment Report: Climate Change (2007) *Pew Center on Global Climate Change*. http://www.pewclimate.org/global-warming-basics/ipccar4.cfm (accessed on 3 January 2010).
2. Lelieveld J, Crutzen PJ, Dentener FJ (2002) Changing concentration, lifetime and climate forcing of atmospheric methane. *Tellus B* 50: 128–150.
3. Hein R, Crutzen PJ, Heimann M (1996) An inverse modeling approach to investigate the global atmospheric methane cycle. *Global Biogeochem Cycles* 11: 43–76.
4. Segers R (1998) Methane production and methane consumption: a review of processes underlying wetland methane fluxes. *Biogeochemistry* 41: 23–51.
5. Dunfield P, Knowles R, Dumont R *et al.* (1993) Methane production and consumption in temperate and subarctic peat soils: response to temperature and pH. *Soil Biol Biochem* 25: 321–326.
6. Linton JD, Vokes J (1978) Growth of the methane utilising-bacterium *Mythylococcus* NCIB 11083 in mineral salts medium with methanol as the sole source of carbon. *FEMS Microbiol Lett* 4: 125–128.
7. Pavlostathis SG, Giraldo-Gomez E (1991) Kinetics of anaerobic treatment. *Water Sci Technol* 24: 35–59.
8. Hilbert DW, Roulet N, Moore T (2000) Modelling and analysis of peatlands as dynamical systems. *J Ecol* 88: 230–242.
9. King GM, Roslev P, Skovgaard H (1990) Distribution and rate of methane oxidation in sediments of the Florida Everglades. *Appl Environ Microbiol* 56: 2902–2911.
10. Kettunen A (2003) Connecting methane fluxes to vegetation cover and water table fluctuations at micro site level: a modeling study. *Global Biogeochem Cycles* 17: 1051–1069.
11. Press WH, Teukolsky S, Vetterling WT *et al.* (2007) *Numerical Recipes: The Art of Scientific Computing*, 3rd ed. Cambridge University Press, Cambridge, UK.
12. Rice JA (1994) *Mathematical Statistics and Data Analysis Second Edition*, Duxbury Press, Pacific Grove, CA.
13. Hosono T, Nouchi I (1997) The dependence of methane transport in rice plants on the root zone temperature. *Plant Soil* 191: 233–240.